Synthetic Approaches to the Molybdenum Site in Nitrogenase. Preparation and Structural Properties of the Molybdenum–Iron–Sulfur "Double-Cubane" Cluster Complexes $[Mo_2Fe_6S_8(SC_2H_5)_9]^{3-}$ and $[Mo_2Fe_6S_9(SC_2H_5)_8]^{3-}$

Thomas E. Wolff,[1a] Jeremy M. Berg,[1a] Keith O. Hodgson,[1a,b] Richard B. Frankel,[1c] and R. H. Holm*[1a]

Contribution from the Department of Chemistry, Stanford University, Stanford, California 94305, and the Francis Bitter National Magnet Laboratory, Massachusetts Institute of Technology, Cambridge, Massachusetts 02139.
Received January 31, 1979

Abstract: A reaction system consisting of $(R_4N)_2MoS_4$, $FeCl_3$, NaOMe, and ethanethiol in methanol affords at least three anionic Mo–Fe–S–SEt cluster complexes. The synthesis, ^{57}Fe Mössbauer spectra in zero applied magnetic field, and X-ray absorption (EXAFS) properties for two of these clusters, $[Mo_2Fe_6S_8(SEt)_9]^{3-}$ and $[Mo_2Fe_6S_9(SEt)_8]^{3-}$, are described. $(Et_3NCH_2Ph)_3[Mo_2Fe_6S_8(SEt)_9]$ (I) and $(Et_4N)_3[Mo_2Fe_6S_9(SEt)_8]$ (II) both crystallize in the hexagonal space group $P6_3/m$ with $Z = 2$. The unit cell of I has the dimensions $a = b = 17.076$ (7) and $c = 16.816$ (5) Å; the structure was refined to $R = 4.8\%$ using 645 unique data with $F_o^2 > 3\sigma(F_o^2)$. The unit cell of II has the dimensions $a = b = 17.230$ (6) and $c = 15.999$ (4) Å; the structure was refined to 5.8% using 800 unique data with $F_o^2 > 3\sigma(F_o^2)$. The structures of both anions consist of two nearly isodimensional pairs of cubane-type $MoFe_3S_4(SEt)_3$ clusters which are triply bridged by sulfur atoms between two six-coordinate Mo atoms. In $[Mo_2Fe_6S_8(SEt)_9]^{3-}$ and $[Mo_2Fe_6S_9(SEt)_8]^{3-}$ the bridging units and Mo···Mo separations are $Mo(\mu_2\text{-}SEt)_3Mo$, 3.668 (4) Å, and $Mo(\mu_2\text{-}S)(\mu_2\text{-}SEt)_2Mo$, 3.306 (3) Å, respectively. A Mo···Mo distance of 3.191 (2) Å was found in triclinic $(Et_3NCH_2Ph)_3[Mo_2Fe_6S_9(SEt)_8]$. The clusters contain $MoFe_3S_4$ cores, similar in shape to those in the ferredoxin site analogues $[Fe_4S_4(SR)_4]^{2-,3-}$ but with a crystallographically imposed trigonal distortion. Interpolation of observed ^{57}Fe isomer shifts with the essentially linear dependence of shifts of tetrahedral FeS_4 units on formal oxidation state leads to a mean $Fe^{2.67+}$ state or a formal 2Fe(III) + Fe(II) description. On this basis $[Mo_2Fe_6S_8(SEt)_9]^{3-}$ contains two $[Mo^{III}Fe_3S_4]^0$ cores and $[Mo_2Fe_6S_9(Et)_8]^{3-}$ a $[Mo^{III}Fe_3S_4]^0$ and a $[Mo^{IV}Fe_3S_4]^+$ core. Isomer shifts of these species (0.27–0.32 mm/s at 4.2–77 K) are similar to that reported for the EPR-active site in the FeMo cofactor of nitrogenase, suggesting a mean oxidation state near $Fe^{2.67+}$ in the latter. Analysis of the extended X-ray absorption fine structure (EXAFS) of the Mo atoms in $[Mo_2Fe_6S_8(SEt)_9]^{3-}$, $[Mo_2Fe_6S_9(SEt)_8]^{3-}$, and nitrogenase is presented and discussed. Curve-fitting procedures afford Mo–S and Mo–Fe distances in the synthetic clusters which are in good agreement with those obtained from X-ray crystallography. EXAFS clearly reflects the structural difference between the symmetrical $Mo(\mu_2\text{-}SEt)_3Mo$ and the unsymmetrical $Mo(\mu_2\text{-}S)(\mu_2\text{-}SEt)_2Mo$ bridging units. Simulation of the EXAFS of the (unsynthesized) linked cubane structure (S_4Fe_3)-$Mo(Fe_3S_4)$ with trigonal symmetry suggests that it is an unlikely model for the Mo site in nitrogenase. Of the two synthetic clusters described here the Mo environment in the unsymmetrically bridged species $[Mo_2Fe_6S_9(SEt)_8]^{3-}$, by the criterion of EXAFS, more closely resembles that in the enzyme.

Introduction

In the last decade, research on the structure, function, and mode of action of molybdenum-containing enzymes,[2-4] and on the potentially biologically relevant inorganic chemistry of molybdenum,[5] has greatly intensified. The structure of biological molybdenum coordination sites, which in most cases are suspected to be the sites of enzymatic catalysis, are largely unknown in any detail, However, recent analyses of the extended X-ray absorption fine structure[6] (EXAFS) of Mo spectra of three enzymes have led to detection of one and probable recognition of another of the four general types of biological coordination sites which have been classified elsewhere.[7] In milk xanthine oxidase[8] and liver sulfite oxidase[9] the Mo atom is found in a mononuclear site as an oxo complex with remaining coordination positions occupied mainly or exclusively by sulfur atoms from protein side chains. The situation in the FeMo proteins of the nitrogenases from *Clostridium pasteurianum*[10] and *Azotobacter vinelandii*[11] and the FeMo cofactor[11] (FeMo-co) isolated from the latter protein[12] is distinctly different. Results of EXAFS analyses[10,11] have led to the following principal conclusions: (1) the Mo coordination sites in the native proteins and in FeMo-co are highly similar or identical; (2) the Mo atom is primarily ligated by sulfur and is separated by <3 Å from another metal, most definitely not Mo and therefore Fe, which is the only other metallic component of nitrogenase;[13] (3) Mo=O interactions are absent in the resting (semireduced) state of the enzyme, and appear only when the enzyme is irreversibly aerobically deactivated. These structural differences deduced from the X-ray absorption data are consistent with observations that the FeMo-co and the "Mo cofactor",[14,15] possibly common to all other molybdoenzymes, are not interchangeable in biochemical assay experiments.[15]

Conclusion (2), together with the known presence of inorganic sulfide and cysteinyl residues in nitrogenase FeMo proteins,[13] implicates Mo in a Mo–Fe–S(R) polynuclear cluster structure with metal bridging by sulfide and, possibly, terminal ligation by cysteinate. Several such structures have been proposed earlier.[10] One of these involves a cubane-type $MoFe_3S_4$ core unit similar to the Fe_4S_4 structures found in ferredoxin protein redox sites and synthetic analogues of these sites.[7,16] Although a few Mo–Fe–S(R) complexes had been reported earlier,[17-20] none appeared to afford the cluster structural features suggested by EXAFS analysis, and thus were not considered as suitable starting points for a synthetic approach to the Mo coordination site in nitrogenase. In executing the approach reported herein we assume the presence in the enzyme of a Mo–Fe–S(R) cluster, supported to an extent by other spectroscopic evidence.[21,22] We have adopted the working hypothesis that this cluster, as $[Fe_4S_4(SR)_4]^{2-}$ site analogues,[7,16] may be a thermodynamically favored soluble

0002-7863/79/1501-4140$01.00/0

Table I. Summary of Crystal Data, Intensity Collection, and Structure Refinement Parameters

data	$(Et_3NCH_2Ph)_3[Mo_2Fe_6S_8(SEt)_9]$	$(Et_4N)_3[Mo_2Fe_6S_9(SEt)_8]$
formula	$C_{57}H_{111}Fe_6Mo_2N_3S_{17}$	$C_{40}H_{100}Fe_6Mo_2N_3S_{17}$
a, Å	17.076 (7)	17.230 (6)
b, Å	17.076 (7)	17.230 (6)
c, Å	16.816 (5)	15.999 (4)
crystal system	hexagonal	hexagonal
V, Å^3	4242 (5)	4113 (2)
Z	2	2
d_{calcd}, g/cm^3	1.49	1.37
d_{obsd}, g/cm^3	1.49[a]	1.47[b]
space group	$P6_3/m$	$P6_3/m$
crystal dimensions,[c] mm	0.22 × 0.18 × 0.10	0.58 × 0.37 × 0.25
crystal faces	$(10\bar{2})$, (001), $(\bar{3}10)$, $(\bar{2}30)$, $(1\bar{1}0)$, (140), $(\bar{2}10)$, $(10\bar{1}0)$	(001), $(00\bar{1})$, $(3\bar{1}0)$, $(\bar{1}10)$, $(\bar{3}10)$, $(\bar{1}\bar{3}0)$
radiation[d]	Mo($\lambda K_{\bar{\alpha}}$ 0.710 69 Å)	Mo($\lambda K_{\bar{\alpha}}$ 0.710 69 Å)
absorption coefficient, μ, cm^{-1}	17.3	17.8
transmission factors, %	74.35 min, 82.88 max, 81.96 av	65.53 min, 69.85 max, 67.95 av
takeoff angle, deg	3.0	3.0
scan speed, deg/min	2.0 to 29.3 ($\theta/2\theta$ scan)	1.0 to 29.3 ($\theta/2\theta$ scan)
scan range, deg	0.7 below $K\alpha_1$ to 0.7 above $K\alpha_2$	0.6 below $K\alpha_1$ to 0.6 above $K\alpha_2$
background/scan time ratio	0.25	0.25
data collected	2θ of 3–50° $+h$, $+k$, $+l$	2θ of 1–50° $+h$, $+k$, $+l$
unique data (F_o^2) > $3\sigma(F_o^2)$	645	800
no. of variables	151	111
error in observation of unit weight	1.54	2.82
R, %	4.8	5.8
R_w, %	5.4	8.7

[a] Determined by flotation in CCl_4 and cyclohexane. [b] Determined by flotation in a solution of p-dibromobenzene in bromobenzene–cyclohexane; absorption of solvent was indicated by density increase with time in this and other solvent mixtures. [c] Irregularly shaped crystal. [d] Mosaic graphite monochromator.

reaction product and hence it, or some precursor of it, may spontaneously self-assemble from simple reactants.

Our first experiments[23] have led to the preparation and structural characterization of the bridged double-cubane complex $[Mo_2Fe_6S_9(SEt)_8]^{3-}$, which contains two $MoFe_3S_4$ cubane-type cores linked by a Mo (μ_2-S)(μ_2-SEt)$_2$Mo bridging unit and whose Mo site by the EXAFS criterion is closely related to that in nitrogenase. Nearly simultaneously, Christou et al.[24,25a] described the structure and several other properties of the related complex $[Mo_2Fe_6S_8(SPh)_9]^{3-}$, which contains a Mo($\mu_2$-SPh)$_3$Mo bridge, but did not disclose its preparation.[25b] Here we report full details of the syntheses and X-ray structures of $[Mo_2Fe_6S_9(SEt)_8]^{3-}$ and $[Mo_2Fe_6S_8(SEt)_9]^{3-}$, certain Mössbauer and X-ray spectroscopic results, and further consideration of the relationship between Mo coordination environments in these clusters and in nitrogenase.

Experimental Section

Preparation of Compounds. The Et_4N^+ and $Et_3NCH_2Ph^+$ salts of tetrathiomolybdate used in the following preparations were obtained by addition of 2.1 equiv of the quaternary ammonium chloride to a slurry of $(NH_4)_2MoS_4$[26] in acetonitrile. After stirring for 2 h under a dinitrogen atmosphere and filtration, the salts were isolated in high yield as bright red, crystalline solids by volume reduction of the filtrate.

General Procedure for Cluster Complexes. All operations were carried out under a pure dinitrogen atmosphere; all solvents were thoroughly degassed prior to use. Three solutions of reactants were prepared as follows: (1) 4.0 g (25 mmol) of anhydrous $FeCl_3$ was dissolved in 100 mL of anhydrous methanol and the solution was filtered through a Celite pad; (2) 5.1 g (83 mmol) of ethanethiol was added to a solution of 4.5 g (83 mmol) of sodium methoxide in 100 mL of anhydrous methanol; (3) 8.3 mmol of tetraalkylammonium tetrathiomolybdate was dissolved in ca. 400 mL of anhydrous methanol and the solution was filtered. In succession, solutions 2 and 3 were added via stainless steel cannulae to solution 1 under continuous stirring. After complete addition of solution 2 the reaction mixture consisted of a greenish solution and a brown precipitate. Over the course of addition of solution 3 the reaction mixture darkened and finally formed an intense brown solution in which was suspended some brownish oily material. This mixture was stirred for 15 h at room temperature. Subsequent workup was dependent upon the desired product.

$(Et_4N)_3[Mo_2Fe_6S_9(SEt)_8]$. Filtration of the reaction mixture afforded 0.6 g of purple residue (which was insoluble in methanol, acetonitrile, and DMF and was not further characterized) and a dark orange-brown filtrate. The brownish residue remaining from evaporation of the filtrate in vacuo was crystallized from a mixture of 75 mL of acetonitrile and 125 mL of THF to yield 3.0 g of black, crystalline material. Four recrystallizations of this material from 2:3 v/v acetonitrile/THF gave 1.6 g (25% based on Mo) of black, crystalline product of acceptable purity by a ^1H NMR criterion (see text). Anal. Calcd for $C_{40}H_{100}Fe_6Mo_2N_3S_{17}$: C, 28.34; H, 5.95; Fe, 19.97; Mo, 11.32; N, 2.48; S, 32.15. Found: C, 28.42; H, 5.95; Fe, 19.18; Mo, 10.93; N, 2.48; S, 32.32. Absorption spectrum (acetonitrile): λ_{max} 268 nm (ϵ_M 50 500), 396 (32 900).

$(Et_3NCH_2Ph)_3[Mo_2Fe_6S_9(SEt)_8]$. Filtration of the reaction mixture gave ca. 1 g of purple-black microcrystals and a dark orange-brown filtrate, which was evaporated to dryness in vacuo. The resultant residue was dissolved in 200 mL of acetonitrile, the solution was filtered to remove insoluble material (mainly sodium chloride), and the orange-brown filtrate was evaporated to dryness in vacuo. Crystallization of the brownish residue from ca. 600 mL of warm ethanol resulted in 2.1 g (28% based on Mo) of black, crystalline product. One recrystallization from ethanol afforded 0.67 g of product considered pure by ^1H NMR and analytical results. Anal. Calcd for $C_{55}H_{106}Fe_6Mo_2N_3S_{17}$: C, 35.11; H, 5.68; Fe, 17.81; Mo, 10.20; N, 2.23; S, 28.97. Found: C, 34.91; H, 5.89; Fe, 17.54; Mo, 9.98; N, 2.11; S, 28.86. Absorption spectrum (acetonitrile): λ_{max} 268 nm (ϵ_M 51 100), 396 (31 300).

$(Et_3NCH_3Ph)_3[Mo_2Fe_6S_8(SEt)_9]$. The reaction mixture, which consisted of a dark orange-brown solution and some suspended microcrystalline solid, was reduced in vacuo to a volume of ca. 250 mL and cooled to −10 to −20 °C for 3 h. Filtration of the cold mixture gave 5.7 g of solid composed of a green material and purple-black microcrystals. Crystallization of this mixture from ca. 75 mL of acetonitrile (in which the green solid (2.1 g) did not dissolve) and ca. 175 mL of THF afforded 1.9 g (24% based on Mo) of black, crystalline product. One recrystallization from acetonitrile/THF gave 0.96 g of product considered pure by ^1H NMR and analytical results. Anal.

Calcd for $C_{57}H_{111}Fe_6Mo_2N_3S_{17}$: C, 35.83; H, 5.86; Fe, 17.54; Mo, 10.04; N, 2.20; S, 28.53. Found: C, 35.84; H, 5.74; Fe, 17.10; Mo, 9.80; N, 2.36; S, 28.43. Absorption spectrum (acetonitrile): λ_{max} 277 nm (ϵ_M 58 200), 391 (36 300). The purple-black microcrystals obtained by the initial filtration in the preceding preparation are identical with this compound.

Collection and Reduction of X-ray Data for $(Et_4N)_3[Mo_2Fe_6S_9(SEt)_8]$ and $(Et_3NCH_2Ph)_3[Mo_2Fe_6S_8(SEt)_9]$. Black, air-sensitive crystals of both compounds, obtained by the crystallization procedures described in the previous section, were transferred under argon and sealed inside glass capillaries. Diffraction studies were carried out on a Syntex $P2_1$ four-circle diffractometer. The machine parameters are summarized in Table I. Fifteen machine-centered reflections whose 2θ values ranged from 12 to 23° were used in the least-squares refinement of the orientation matrix and the lattice parameters for the two crystals. Suitable mosaicity for data collection of both crystals was indicated by ω scans of five low-angle reflections for each crystal; the scans gave full width at half-maximum of less than 0.25° in all cases.

The parameters utilized in intensity collection are summarized in Table I. Throughout each data collection three standards were collected, and in no case was any significant variation in intensities observed. Inspection of the intensity data and of partial rotation photographs did not allow unambiguous determination of the space group of the two crystals. Each data set showed only the systematic absence $000l$, $l = 2n$, which was consistent with space groups $P6_3$, $P6_3/m$, or $P6_322$. Statistical analyses of the intensity data suggested a centric space group in both cases. Subsequent refinement of both structures in $P6_3/m$ confirmed this choice as correct. The intensity data sets were processed using the program ENXDR, as described previously.[27] Numerical analytical absorption corrections were applied to both data sets to account for the irregular shapes of the crystals.

Solution and Refinement of the Structures. The two structures were solved in a straightforward manner with the direct-methods program MULTAN. Using 263 and 185 normalized structure factors for $[Mo_2Fe_6S_9(SEt)_8]^{3-}$ and $[Mo_2Fe_6S_8(SEt)_9]^{3-}$, respectively, 32 phase sets were generated. The presence of two formula units per cell in space group $P6_3/m$ suggested that the anions were situated along the threefold axes and across the mirror planes at $z = 1/4$ and $z = 3/4$. In this case the asymmetric unit consists of one-sixth of the anion and one-half of the cation. For both structures the phase set with the highest absolute figure of merit yielded trial positions for all Mo, Fe, and S atoms.

Difference Fourier methods were applied to locate the remaining nonhydrogen atoms in each structure. For $(Et_4N)_3[Mo_2Fe_6S_9(SEt)_8]$, inspection of the difference Fourier map clearly revealed the positions of the cation atoms, but the regions of electron density around the methyl carbon atoms of the Fe-SEt groups and in the region of the bridge between the two molybdenum atoms were not uniquely defined. The maps of the bridging region revealed electron density elongated in the mirror plane and attributable to sulfur atoms. Moreover, additional density indicated the presence of an ethyl group with partial occupancy near a sulfur atom. The bridge region thus appeared to contain sulfur atoms from both sulfide and thiolate groups (a matter substantiated by EXAFS analysis, vide infra). Two apparently different distances from the Mo atom to the disordered S atoms in the mirror plane could not be resolved because of the resolution limit of the data. The disorder was modeled by allowing one S atom to refine anisotropically; this atom assumed a root mean square amplitude of ~0.55 Å^2 in the mirror plane with density extending toward the ethyl group. Separate refinement cycles were then carried out with the occupancies of the ethyl C atoms set as if there were either one or two ethyl groups distributed by the threefold axis over the three bridging positions. The isotropic thermal parameters for the methylene carbon atoms were ~5.0 and ~1.0 Å^2 for the cases of two and one ethyl groups in the bridging region, respectively. The more reasonable value of 5.0 Å^2 was taken to indicate that two ethyl groups are distributed over three bridging positions. Thus, the bridge electron density was satisfactorily described and refined in terms of the $Mo(\mu_2\text{-}S)(\mu_2\text{-}SEt)_2Mo$ unit whose bridging groups are disordered by the crystallographic threefold axis. Inspection of the difference Fourier map following inclusion of the bridging atoms revealed two positions for the Fe-SEt methyl C atoms. The occupancy of this twofold disordered methyl group was described by assigning the occupancy factors of x and $(1 - x)$ for the two positions. Refinement of x led to a 2:1 ratio in the different positions of the methyl C atom. These two positions are labeled C(2)S(4) and C(3)S(4) in the tables which follow.

In contrast to the sulfur atom bridge disorder in $(Et_4N)_3[Mo_2Fe_6S_9(SEt)_8]$, the difference Fourier map showed a well-defined position for the bridging S atom in the structure of $(Et_3NCH_2Ph)_3[Mo_2Fe_6S_8(SEt)_9]$. This atom refined with full occupancy to give reasonable thermal parameters showing no abnormal elongation in the mirror plane. The methylene C atom of each of the bridging SEt groups was found to be in the mirror plane and was ordered. The methyl C atoms of each such group were disordered into two mirror-related positions. This methyl C atom is labeled C(2)S(3) in the tables and the second position for the methyl C atom of the bridging SEt group is generated by the mirror operation. The electron density in the region of the Fe-SEt groups was found to contain three possible positions for the methyl C atom. Least-squares constraints were set up to allow the occupancy factor to vary, distributing the methyl group over the three positions such that the sum of the occupancies was one. This refinement yielded occupancy factors of 0.31, 0.20, and 0.49 for atoms labeled C(2)S(4), C(3)S(4), and C(4)S(4), respectively, in the tables.

Refinement of both structures, treating the disorder problems using derivative constraints as described above, was by full-matrix least-squares methods. The procedures and sources of atomic scattering factors have been given previously.[27] The final least-squares cycles included hydrogen atoms of the cations; C-H distances and hydrogen atom isotropic temperature factors were set at 0.95 Å and 7 Å^2, respectively. The final R factors are given in Table I. For each structure the highest peak in the final difference Fourier map was ~25% of the height of a carbon atom peak. This low residual electron density is distributed more or less randomly throughout the map, indicating that the disorder problems were well described in the final refinements.

The following results for $(Et_3NCH_2Ph)_3[Mo_2Fe_6S_8(SEt)_9]$ and $(Et_4N)_3[Mo_2Fe_6S_9(SEt)_8]$ are tabulated: positional and thermal parameters for the anions (Table II) and the cations (Table VI);[28] interatomic distances and angles in the anions (Table III) and the cations (Table VII);[28] the best weighted least-squares planes for the anions (Table IV); root mean square amplitudes of thermal vibration of the anions (Table V); calculated hydrogen atom positions in the cations (Table VIII);[28] values of $10|F_o|$ and $10|F_c|$ (Tables IX and X[28]). Structures of the two anions are presented in Figures 1 and 2.

The crystal structure of $(Et_3NCH_2Ph)_3[Mo_2Fe_6S_9(SEt)_8]$ has also been solved by the procedures described. The compound crystallizes in the triclinic space group $P\bar{1}$ with one anion and three cations in the asymmetric unit and the following unit cell dimensions: a = 15.948 (6) Å, b = 19.005 (9) Å, c = 15.675 (8) Å, α = 98.09 (4)°, β = 117.25 (3)°, γ = 89.25 (3)°. Despite the fact that no symmetry is imposed on the anion, the crystallographic disorder of bridging thiolate and sulfide groups persists. Additionally, one of the cations exhibits substantial disorder. With the exception of methyl carbon atoms of the bridging thiolate groups, all nonhydrogen atoms were located. The structure was refined to R = 9.0%, R_w = 13.4% using 4557 reflections with $F_o^2 > 3\sigma(F_o^2)$. The configuration and dimensions of the anion are very similar to those in its Et_4N^+ salt. With reference to Figure 2 the following *average* distances were found: Mo···Fe, 2.741 (10) Å; Mo-S(1), 2.347 (8) Å; Fe···Fe, 2.701 (9) Å; Fe-S (1), 2.259 (6) Å; Fe-S (2), 2.278 (13) Å; Fe-S (4), 2.232 (16) Å. The most significant structural feature is the Mo···Mo distance of 3.191 (2) Å, substantially shorter than that in the Et_4N^+ salt. Because of the similarity of the anions in the two compounds, further structural details of the $(Et_3NCH_2Ph)^+$ salt are not included.

EXAFS Data Collection and Analysis. All X-ray absorption spectra were recorded at the Stanford Synchrotron Radiation Laboratory. The experimental apparatus has been described previously.[10,29] The Mo Kα absorption spectra reported herein were measured in the transmission mode using a channel-cut Si[2,2,0] monochromator crystal and Ar-filled ionization detectors. The data collection for the FeMo protein of nitrogenase from *Clostridium pasteurianum* has been described in an earlier paper.[10] The spectrum of $[Mo_2Fe_6S_8(SEt)_9]^{3-}$ was taken at moderately low beam energy (2.6 GeV and 12 mA average current) and the final spectrum is the average of four 25-min scans. The spectrum of $[Mo_2Fe_6S_9(SEt)_8]^{3-}$ was recorded at high energy and is the average of two 15-min scans. All spectra were recorded under anaerobic conditions.

The data processing and analysis were carried out as described in earlier reports on synthetic molybdenum complexes[29] and nitrogenase.[10] The curve-fitting analysis utilized nonlinear least squares to

Table II. Positional and Thermal Parameters for Anions

atom	x	y	z	β_{11}[a]	β_{22}	β_{33}	β_{12}	β_{13}	β_{23}
				$(Et_3NCH_2Ph)_3[Mo_2Fe_6S_8(SEt)_9]$					
Mo	0.3333 (0)[b]	0.6667 (0)	0.1408 (1)	0.003 67 (9)	0.0037 (0)	0.002 39 (7)	0.0034 (0)	0.0000 (0)	0.0000 (0)
Fe	0.2624 (1)	0.5643 (1)	0.0076 (1)	0.005 13 (8)	0.005 06 (9)	0.002 92 (6)	0.0050 (1)	−0.0007 (2)	−0.0011 (2)
S(1)	0.3769 (2)	0.5703 (2)	0.0799 (2)	0.0045 (1)	0.0046 (1)	0.0032 (1)	0.0049 (2)	0.0002 (3)	0.0000 (3)
S(2)	0.3333 (0)	0.6667 (0)	−0.0913 (4)	0.0077 (5)	0.0077 (0)	0.0026 (2)	0.0069 (0)	0.0000 (0)	0.0000 (0)
S(3)	0.2986 (3)	0.7501 (3)	0.2500 (0)	0.0044 (2)	0.0042 (2)	0.0027 (2)	0.0041 (3)	0.0000 (0)	0.0000 (0)
S(4)	0.1713 (3)	0.4333 (3)	−0.0530 (3)	0.0077 (2)	0.0086 (2)	0.0089 (3)	0.0080 (3)	−0.0052 (5)	−0.0089 (5)
C(1)S(3)[c]	0.1760 (11)	0.7149 (11)	0.2500 (0)	0.0034 (7)	0.0038 (7)	0.0043 (9)	0.0051 (10)	0.000 (0)	0.000 (0)
C(2)S(3)	0.1647 (19)	0.7874 (19)	0.2050 (20)	0.0084 (15)	0.0101 (16)	0.0099 (25)	0.0136 (20)	−0.004 (3)	0.002 (3)
C(1)S(4)	0.1148 (17)	0.3480 (17)	0.0088 (15)	0.0266 (22)	0.0179 (18)	0.0100 (12)	0.0247 (25)	0.014 (3)	0.001 (3)
C(2)S(4)	0.203 (3)	0.315 (3)	0.057 (3)	5. (1)					
C(3)S(4)	0.143 (3)	0.354 (4)	0.071 (3)	3. (1)					
C(4)S(4)	0.025 (2)	0.275 (2)	−0.053 (2)	8 (1)					
				$(Et_4N)_3[Mo_2Fe_6S_9(SEt)_8]$					
Mo	0.3333 (0)	0.6667 (0)	0.1467 (1)	0.004 64 (9)	0.0046 (0)	0.003 86 (9)	0.0046 (0)	0.0000 (0)	0.0000 (0)
Fe	0.2613 (1)	0.5651 (1)	0.0066 (1)	0.005 61 (8)	0.005 26 (8)	0.004 41 (8)	0.0053 (1)	−0.0005 (2)	−0.0008 (2)
S(1)	0.3732 (2)	0.5690 (2)	0.0836 (2)	0.0058 (1)	0.0054 (1)	0.0049 (2)	0.0063 (2)	0.0003 (3)	0.0001 (3)
S(2)	0.3333 (0)	0.6667 (0)	−0.0975 (4)	0.0071 (4)	0.0071 (0)	0.0034 (2)	0.0067 (0)	0.0000 (0)	0.0000 (0)
S(3)	0.3038 (7)	0.7447 (6)	0.2500 (0)	0.0133 (6)	0.0126 (6)	0.0070 (3)	0.0083 (9)	0.0000 (0)	0.0000 (0)
S(4)	0.1690 (3)	0.4326 (3)	−0.0534 (3)	0.0077 (2)	0.0067 (2)	0.0088 (3)	0.0056 (3)	−0.0023 (5)	−0.0049 (4)
C(1)S(4)[c]	0.1412 (20)	0.3530 (14)	0.027 (2)	0.0236 (28)	0.0060 (13)	0.0148 (18)	0.0003 (29)	0.014 (4)	−0.004 (3)
C(1)S(3)	0.239 (2)	0.772 (2)	0.250 (0)	5.0 (7)					
C(2)S(3)	0.174 (3)	0.718 (3)	0.250 (0)	9.0 (12)					
C(2)S(4)	0.092 (3)	0.262 (3)	−0.002 (3)	16.6 (16)					
C(3)S(4)	0.157 (6)	0.297 (5)	0.018 (5)	15.3 (30)					

[a] The form of the anisotropic thermal ellipsoid is $\exp[-(\beta_{11}h^2 + \beta_{22}k^2 + \beta_{33}l^2 + \beta_{12}hk + \beta_{13}hl + \beta_{23}kl)]$. [b] Estimated standard deviations in parentheses in this and succeeding tables. [c] Numbering scheme: bridge, S(3)-C(1)-C(2); terminal, S(4)-C(1)-C(2,3,4). C(2), C(3), C(4) refer to the disordered β-C atoms of the terminal thiolate ligands (cf. footnotes *a* and *b*, Table III).

Table III. Selected Interatomic Distances (Å) and Angles (deg) in Anions

distance/angle	$(Et_3NCH_2Ph)_3[Mo_2Fe_6S_8(SEt)_9]$	$(Et_4N)_3[Mo_2Fe_6S_9(SEt)_8]$
Mo···Mo	3.668 (4)	3.306 (3)
Mo···Fe	2.723 (2)	2.730 (2)
Fe···Fe	2.687 (3)	2.702 (2)
Mo-S(1)	2.351 (3)	2.340 (3)
Mo···S(2)	3.899 (7)	3.907 (4)
Mo-S(3)	2.567 (4)	
Fe-S(1)	2.249 (4)	2.261 (3)
Fe-S(1)	2.259 (4)	2.264 (3)
Fe-S(2)	2.273 (5)	2.282 (3)
Fe-S(4)	2.232 (5)	2.243 (3)
S(1)···S(1)	3.667 (6)	3.658 (4)
S(1)···S(2)	3.571 (6)	3.586 (4)
S(3)···S(3)	3.111 (9)	
S(3)-C(1)	1.866 (18)	
S(4)-C(1)	1.651 (28)	1.762 (22)
C(1)S(3)-C(2)S(3)	1.543 (33)	
C(1)S(4)-C(2)S(4)	2.023 (57)[a]	1.439 (38)[b]
C(1)S(4)-C(3)S(4)	1.131 (58)[a]	1.137 (78)[b]
C(1)S(4)-C(4)S(4)	1.761 (46)[a]	
S(1)-Mo-S(3)	89.18 (14), 90.36 (14)	
S(3)-Mo-S(3)	74.59 (13)	
S(1)-Mo-S(1)	102.47 (11)	102.80 (8)
S(1)-Fe-S(1)	108.86 (18)	107.88 (14)
S(1)-Fe-S(2)	104.01 (13), 104.33 (13)	104.16 (10), 104.26 (10)
S(1)-Fe-S(4)	115.85 (18), 116.41 (18)	115.09 (13), 116.43 (12)
S(2)-Fe-S(4)	105.90 (21)	107.77 (12)
Mo-S(1)-Fe	72.38 (12), 72.55 (12)	72.72 (9), 72.78 (9)
Fe-S(1)-Fe	73.17 (14)	73.32 (10)
Fe-S(2)-Fe	72.47 (18)	72.59 (12)
Mo-S(3)-Mo	91.20 (17)	
Mo-S(3)-C(1)S(3)	110.76 (36)	
Fe-S(4)-C(1)S(4)	113.8 (1.4)	104.9 (6)
Fe···Mo···Fe	59.12 (8)	59.30 (5)
Fe···Fe···Fe	60.00 (0)	60.00 (0)
Mo···Fe···Fe	60.44 (4)	60.35 (3)
S(1)···S(1)···S(1)	60.00 (0)	60.00 (0)
S(1)···S(1)···S(2)	59.11 (6)	59.34 (5)
S(1)···S(2)···S(1)	61.78 (13)	61.33 (9)
S(3)-C(1)S(3)-C(2)S(3)	108.2 (1.6)	
S(4)-C(1)S(4)-C(2)S(4)	108.2 (2.4)	113.4 (2.1)
S(4)-C(1)S(4)-C(3)S(4)	117.7 (4.7)	118.5 (4.5)
S(4)-C(1)S(4)-C(4)S(4)	99.8 (2.5)	

[a,b] Occupancy factor refinement of β-carbon atoms resulted in these multiplicities: [a] C(2)S(4), 0.31; C(3)S(4), 0.20; C(4)S(4), 0.49; [b] C(2)S(4), 0.67; C(3)S(4), 0.33.

Table IV. Best Weighted Least-Squares Planes for Anions

plane no.	$Ax + By + Cz = D$ (orthogonalized coordinates)			
	A	*B*	*C*	*D*
		$(Et_3NCH_2Ph)_3[Mo_2Fe_6S_8(SEt)_9]$		
1	0.1711	0.7912	−0.5872	6.3890
2	0.5918	−0.5436	−0.5951	−4.7266
3	0.9768	−0.2143	−0.0010	−2.1154
4	0.5269	0.1669	−0.8334	1.1106
		$(Et_4N)_3[Mo_2Fe_6S_9(SEt)_8]$		
1	0.1909	0.7872	−0.5865	6.4299
2	0.5846	−0.5559	−0.5910	−4.8846
3	0.9719	−0.2353	0.0002	−2.3400
4	0.5347	0.1574	−0.8302	1.0434

atom	deviations (Å) from plane no.			
	1	2	3	4
		$(Et_3NCH_2Ph)_3[Mo_2Fe_6S_8(SEt)_9]$		
Mo	0.022 (1)		0.001 (1)	
Fe[a]	0.78 (2)	−0.084 (2)	−0.002 (2)	0.002 (2)
Fe[a]		−0.084 (2)		−0.002 (2)
S(1)[a]	−0.233 (4)	0.267 (4)	−0.004 (4)	0.004 (4)
S(1)[a]	−0.233 (4)			−0.004 (4)
S(2)		0.282 (4)	0.005 (1)	
		$(Et_4N)_3[Mo_2Fe_6S_9(SEt)_8]$		
Mo	0.024 (1)		0.000 (1)	
Fe[a]	0.074 (2)	−0.078 (2)	0.000 (2)	0.000 (2)
Fe[a]		−0.078 (2)		0.000 (2)
S(1)[a]	−0.240 (4)	0.268 (4)	−0.001 (4)	0.001 (4)
S(1)[a]	−0.240 (4)			−0.001 (4)
S(2)		0.278 (4)	0.001 (1)	

[a] Fe and S(1) atom pairs are atoms in the $MoFe_3S_4$ core which are related by threefold symmetry.

Table V. Root Mean Square Amplitudes of Thermal Vibration (Å) of Anions

atom	min	int	max
	$(Et_3NCH_2Ph)_3[Mo_2Fe_6S_8(SEt)_9]$		
Mo	0.185	0.199	0.208
Fe	0.197	0.240	0.243
S(1)	0.211	0.220	0.228
S(2)	0.191	0.286	0.306
S(3)	0.197	0.215	0.223
S(4)	0.228	0.297	0.412
C(1)S(3)	0.152	0.215	0.248
C(2)S(3)	0.192	0.347	0.395
C(1)S(4)	0.292	0.434	0.586
C(2)S(4)[a]	0.241		
C(3)S(4)	0.180		
C(4)S(4)	0.324		
	$(Et_4N)_3[Mo_2Fe_6S_9(SEt)_8]$		
Mo	0.224	0.229	0.229
Fe	0.231	0.250	0.254
S(1)	0.232	0.251	0.259
S(2)	0.209	0.281	0.292
S(3)	0.302	0.358	0.445
S(4)	0.242	0.316	0.361
C(1)S(3)	0.251		
C(2)S(3)	0.338		
C(1)S(4)[a]	0.251	0.374	0.657
C(2)S(4)	0.458		
C(3)S(4)	0.440		

[a] Cf. footnotes *a* and *b*, Table III.

fit the functional form described in these references to the observed EXAFS data. Each shell of atom neighbors is characterized by a damped, amplitude-modulated sine wave and analysis of the overall amplitude provides the number of atoms in the shell while analysis of the linear component of the phase provides the distance. The pairwise phase shift and amplitude parameters (c_1, c_2, a_0, and a_2) for Mo-S were determined semiempirically and were taken from previous

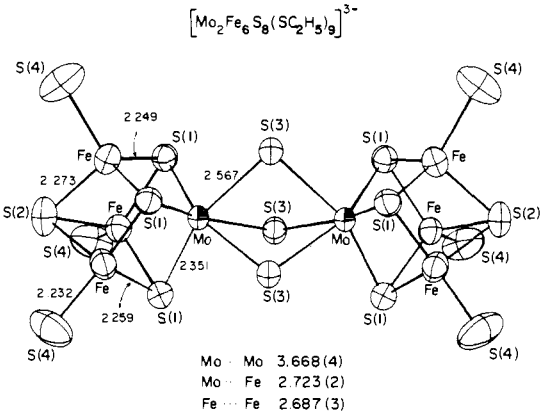

Figure 1. Structure of $[Mo_2Fe_6S_8(SEt)_8]^{3-}$, showing 50% probability ellipsoids, the atom labeling scheme, and principal interatomic distances; not included are the nine ethyl groups of the bridging and terminal thiolate ligands.

work.[29] As pointed out elsewhere[10] the amplitude and phase parameters for Mo-Fe were extrapolated from the Mo-S parameters and known elemental trends. As a suitable single-shell model for determining these Mo-Fe parameters semiempirically is still not available, the extrapolated parameters have been normalized by fitting a Mo-Fe shell which has been Fourier filtered from a species ($[Mo_2Fe_7S_8(SEt)_{12}]^{3-}$), containing a $MoFe_3S_4$ core, whose structure has been accurately determined.[30] The resultant parameters gave improved reliability in the determination of numbers of scattering atoms and made little difference in the distances (which were very accurate even using the extrapolated parameters).

Other Physical Measurements. All measurements were made under anaerobic conditions. Absorption spectra were recorded on a Cary Model 219 spectrophotometer. Mössbauer spectra were obtained with a constant-acceleration spectrometer with the source (^{57}Co in Rh) maintained at the same temperature as the absorber, eliminating the second-order Doppler shift. $(Et_4N)_3[Mo_2Fe_6S_9(SEt)_8]$ and

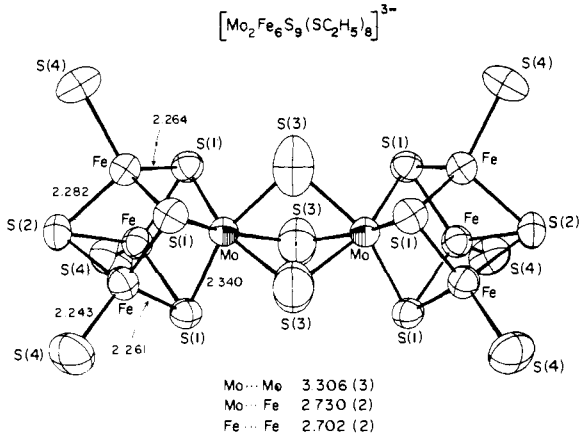

Figure 2. Structure of $[Mo_2Fe_6S_9(SEt)_8]^{3-}$, showing 50% probability ellipsoids, the atom labeling scheme, and principal interatomic distances; not included are the two ethyl groups of the disordered bridge and the six ethyl groups of the terminal thiolate ligands.

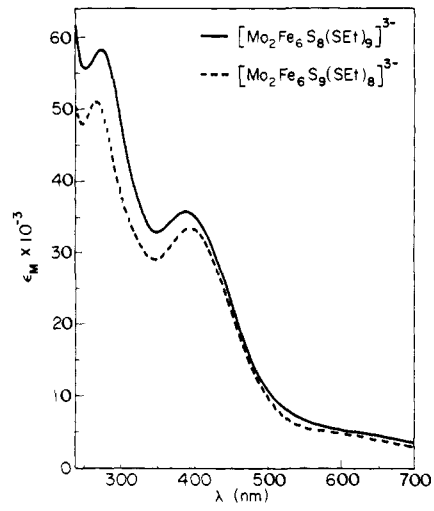

Figure 3. Absorption spectra of $[Mo_2Fe_6S_8(SEt)_9]^{3-}$ and $[Mo_2Fe_6S_9(SEt)_8]^{3-}$ in acetonitrile solution at ~25 °C.

$(Et_3NCH_2Ph)_3[Mo_2Fe_6S_8(SEt)_9]$ were examined at 4.2 and 77 K as solid absorbers dispersed in boron nitride powder.

Results and Discussion

Preparation of Mo–Fe–S Cluster Complexes. After preliminary experimentation, reaction system 1 was devised. This

$$(R_4N)_2MoS_4 + 3FeCl_3 + 10EtSH + 10NaOMe \xrightarrow{MeOH,\ \sim 25\ ^\circ C} (R_4N)_3[Mo_2Fe_6S_9(SEt)_8] + (R_4N)_3[Mo_2Fe_6S_8(SEt)_9] + (R_4N)_3[Mo_2Fe_7S_8(SEt)_{12}] \quad (1)$$

system has afforded three anionic cluster complexes which have been isolated as quaternary ammonium salts and identified. The complexes $[Mo_2Fe_6S_9(SEt)_8]^{3-}$ and $[Mo_2Fe_6S_8(SEt)_9]^{3-}$ are the subjects of this report. The system resembles that which resulted in spontaneous self-assembly of the ferredoxin active site analogues $[Fe_4S_4(SR)_4]^{2-}$ [16,31] except that, in place of NaHS, MoS_4^{2-} is the source of sulfide. Excess thiolate is the apparent reductant required to adjust the oxidation states of iron and molybdenum to those necessary for stable cluster formation.

The reaction system 1 products $[Mo_2Fe_6S_9(SEt)_8]^{3-}$ and $[Mo_2Fe_6S_8(SEt)_9]^{3-}$ were separated on the basis of differential solubilities of certain of their quaternary ammonium salts in alcohols and acetonitrile. Salts of both anions were isolated as black, crystalline, air-sensitive materials. With $(Et_3NCH_2Ph)^+$ as the counterion the $[Mo_2Fe_6S_8(SEt)_9]^{3-}$ salt proved to be the less soluble in methanol. Consequently, substantial quantities of crude $(Et_3NCH_2Ph)_3[Mo_2Fe_6S_8(SEt)_9]$ were isolated by volume reduction of the unfiltered methanol reaction mixture followed by cooling. Purification of this compound was effected by recrystallization from acetonitrile/THF. Filtration of the reaction mixture, extraction of the solid residue obtained from evaporation of the filtrate with acetonitrile, and evaporation of the acetonitrile solution gave a solid residue consisting of the preceding compound and $(Et_3NCH_2Ph)_3[Mo_2Fe_6S_9(SEt)_8]$. The latter was obtained in pure form by two fractional crystallizations from warm ethanol. The Et_4N^+ salts of the two anions have nearly equal solubilities in methanol. Evaporation of the filtrate of the methanol reaction mixture followed by recrystallization of the resultant residue five times from acetonitrile/THF gave a satisfactorily pure sample of $(Et_4N)_3[Mo_2Fe_6S_9(SEt)_8]$. In view of the greater ease in obtaining the corresponding $(Et_3NCH_2Ph)^+$ salt, a purification method for this compound has not been optimized. For the same reason the isolation of $(Et_4N)_3[Mo_2Fe_6S_8(SEt)_9]$ was not pursued.

Product purity was monitored by ^1H NMR spectroscopy, which revealed certain diagnostic signals shifted by paramagnetic interactions from the region of cation resonances. In acetonitrile-d_3 solution (~31 °C) the spectrum of $[Mo_2Fe_6S_8(SEt)_9]^{3-}$ contained broad signals at 54 and 17 ppm downfield of Me_4Si which, on the basis of relative intensities and the X-ray structure (Figure 1) described in a following section, are assigned to terminal $FeSCH_2$ and $Mo(\mu_2\text{-}SCH_2)Mo$ groups, respectively. Similarly, the signals of $[Mo_2Fe_6S_9(SEt)_8]^{3-}$ (Figure 2) at 54 ppm downfield and 3.1 ppm upfield of Me_4Si are attributed to terminal and bridging thiolate methylene groups, respectively. The multiple recrystallizations of $(Et_4N)_3[Mo_2Fe_6S_9(SEt)_8]$ were required to diminish contamination with the $[Mo_2Fe_6S_8(SEt)_9]^{3-}$ salt, whose presence in impure samples was indicated by a signal at 17 ppm. The absorption spectra of $[Mo_2Fe_6S_8(SEt)_9]^{3-}$ (λ_{max} 277, 391 nm) and $[Mo_2Fe_6S_9(SEt)_8]^{3-}$ (λ_{max} 268, 396 nm) in acetonitrile solution are shown in Figure 3. Their similarity renders them less useful than ^1H NMR spectra in monitoring product purity, especially in early stages of purification. These spectra resemble those of $[Fe_4S_4(SEt)_4]^{2-}$ in aprotic solvents (e.g., in DMF[32] λ_{max} 298 nm (ϵ_M 23 300), 420 (17 200)) in that they contain two principal absorption bands. The visible bands in Figure 3 have $\epsilon_{M/2}$ values (i.e., per $MoFe_3S_4$ core, vide infra) similar to those of $[Fe_4S_4(SEt)_4]^{2-}$. The two bands presumably arise from EtS → core charge transfer excitations, analogous to assignment of the two intense bands in the UV-visible spectra of $[Fe_4S_4(SR)_4]^{2-}$ complexes.[16,33] Spectroscopic and other physicochemical properties of $[Mo_2Fe_6S_8(SEt)_9]^{3-}$ and $[Mo_2Fe_6S_9(SEt)_8]^{3-}$ will be considered more fully in a subsequent report.

Description of Structures. Both $(Et_3NCH_2Ph)_3[Mo_2Fe_6S_8(SEt)_9]$ and $(Et_4N)_3[Mo_2Fe_6S_9(SEt)_8]$ crystallize in the hexagonal space group $P6_3/m$ and contain one-sixth of the anion and one-half of the cation in the asymmetric unit. Cations and anions are well separated with no unusually close contacts. The cations of both compounds lie on the mirror planes at $z = 1/4$ and $z = 3/4$, possess unexceptional bond distances and angles (Table VII[28]), and are not disordered. The structures of the two anions, together with the common atom labeling scheme and principal bond distances, are set out in Figures 1 and 2. A stereoview of the structure of $[Mo_2Fe_6S_8(SEt)_9]^{3-}$ is provided in Figure 4. Both anions contain two $MoFe_3S_4(SEt)_3$ clusters bridged through the Mo atoms by three atoms S(3) which are situated on the mirror plane at z

Table XI. Comparison of Mean Values of Selected Distances (Å)

complex	Fe-S	Fe-S*	Fe···Fe	S*···S*	ref
$[Mo_2Fe_6S_8*(SEt)_9]^{3-}$	2.232 (5)	2.260 (10)	2.687 (3)	3.619 (53)	*a*
$[Mo_2Fe_6S_9*(SEt)_8]^{3-}$	2.243 (3)	2.269 (10)	2.702 (2)	3.622 (39)	*a*
$[Fe_4S_4*(SCH_2Ph)_4]^{2-}$ [b]	2.251 (3)	2.286 (35)[d]	2.746 (24)[e]	3.606 (31)[e]	31
$[Fe_4S_4*(SPh)_4]^{2-}$ [b]	2.263 (3)	2.287 (17)[d]	2.736 (3)	3.611 (32)[e]	34
$[Fe_4S_4*(SCH_2CH_2CO_2)_4]^{6-}$ [b]	2.250 (3)	2.287 (19)[d]	2.755 (18)[e]	3.602 (9)[e]	35
$[Fe_4S_4*(SCH_2Ph)_4]^{3-}$ [c]	2.297 (12)	2.317 (15)[f]	2.759 (24)	3.665 (30)[e]	36
$[Fe_4S_4*(SPh)_4]^{3-}$ [c,i]	2.295 (4)	2.309 (35)[g]	2.743 (15)	3.657 (52)[h]	37

[a] This work. [b,c] Core oxidation level: [b] $[Fe_4S_4*]^{2+}$, $Fe^{2.5+}$; [c] $[Fe_4S_4*]^{+}$, $Fe^{2.25+}$. [d-h] Mean value of [d] four short + eight long, [e] four short + two long, [f] six short + six long, [g] eight short + four long, [h] two short + four long distances. The large esd values in Fe-S*, Fe···Fe, and S*···S* distances arise because all such distances were included in calculations of the mean values given. [i] Anion 1.

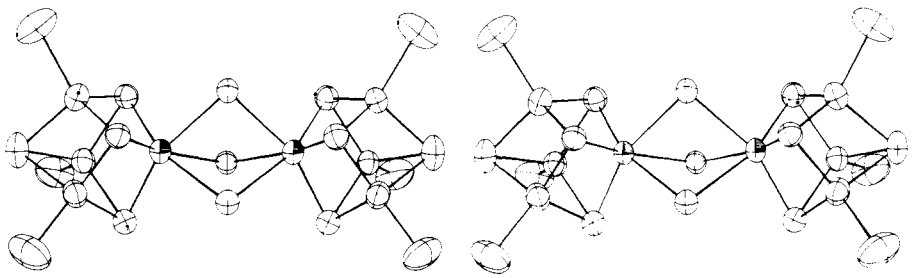

Figure 4. Stereoview of $[Mo_2Fe_6S_8(SEt)_9]^{3-}$; 50% probability ellipsoids are plotted and ethyl groups are omitted.

= 1/4. The anion of each structure lies with its longest intercore dimension, S(2)···S(2), along the crystallographic threefold axis at $x = 1/3$, $y = 2/3$. Other than small dimensional differences the two anions are distinguished by the composition of their bridging units: $Mo(\mu_2\text{-}SEt)_3Mo$ in $[Mo_2Fe_6S_8(SEt)_9]^{3-}$ and $Mo(\mu_2\text{-}S)(\mu_2\text{-}SEt)_2Mo$ in $[Mo_2Fe_6S_9(SEt)_8]^{3-}$. In describing the structures of the anions, clusters and bridging units are considered in turn, and attention is directed to the metrical data in Table III and the best weighted least-squares planes and atom position deviations therefrom in Table IV.

A. $MoFe_3S_4(SEt)_3$ Clusters. The basic cubane-type stereochemistry of the $MoFe_3S_4$ cores of the clusters in the two anions is immediately apparent from inspection of Figures 1, 2, and 4. In this sense these clusters are related to ferredoxin active site synthetic analogues with Fe_4S_4 cores; selected bond distances for five such analogues[31,34-37] are compared with corresponding distances in $[Mo_2Fe_6S_8(SEt)_9]^{3-}$ and $[Mo_2Fe_6S_9(SEt)_8]^{3-}$ in Table XI. The following are the principal cluster structural features in the latter two anions. (1) Owing to crystallographically imposed constraints, the two clusters within each anion are identical and each possesses trigonal symmetry with the C_3 axis passing through Mo and S(2). (2) The $MoFe_3S_4$ cores are composed of two interpenetrating imperfect tetrahedra ($MoFe_3$, S_4) of which the S_4 tetrahedron is the larger. (3) In each structure plane 3 (Table IV), defined by Mo, Fe, S(1), and S(2), is nearly perfect; moreover, in both cases the two independent Fe-S(1) distances are within 3σ of each other. (4) The core faces $MoFeS_2$ and Fe_2S_2 are distinctly nonplanar kite-shaped quadrilaterals (planes 1 and 2); body diagonal planes 4 are nearly perfect. (5) From (1)-(4) the local core symmetry closely approaches C_{3v}. (6) Values of Fe···Fe, Fe-S(1), and Fe-S(4) distances are comparable to those in complexes with Fe_4S_4 cores in several different oxidation levels (Table XI). While direct comparison is not precise owing to distortions of the latter from cubic toward tetragonal[38] rather than trigonal symmetry, the shorter Fe-S(1) and Fe-S(4) distances observed in the $MoFe_3S_4(SEt)_3$ clusters are consistent with a formal oxidation state of Fe higher than those in the tabulated Fe_4S_4 species (vide infra). (7) The increase of 0.17-0.18 Å in Mo-S distances in $MoFe_3S_4$ cores compared to MoS_4^{2-} [39] suggests that the multiple bonding presumably present in the latter species[40] has been substantially diminished, very likely as a consequence of reduction in the formal valence state of Mo and concomitant increase in coordination number. Further assessment of the core Mo-S distances is difficult because of the paucity of lower valent six-coordinate Mo compounds containing triply bridging sulfide. The only prior example is MoS_2, in which the Mo-S distance is 2.41 (6) Å.[41] The Mo(III)-S distance of 2.37 Å in $[Mo_2(\mu_2\text{-}S)_2(CN)_8]^{6-}$ [42] compares favorably with the Mo-S(1) distances of 2.351 (3) and 2.340 (3) Å found for $[Mo_2Fe_6S_8(SEt)_9]^{3-}$ and $[Mo_2Fe_6S_9(SEt)_8]^{3-}$, respectively. A number of binuclear Mo(V) complexes containing one or two sulfide bridges have been structurally characterized; Mo-S distances occur in the 2.29-2.34-Å interval.[43] Mo-S distances and all other core dimensions do not differ significantly from those reported recently for $[Mo_2Fe_6S_8(SPh)_9]^{3-}$ [25a]

B. Bridging Units. The primary structural difference between $[Mo_2Fe_6S_8(SEt)_9]^{3-}$ and $[Mo_2Fe_6S_9(SEt)_8]^{3-}$ is found in the bridging units **1** and **2**, respectively, and the accompanying 0.36-Å difference in Mo···Mo distances. The following are the principal structural features of these two units (excluding the ethyl group disorders discussed in the Experimental Section). (1) Atoms S(3) are related by a crystallographic threefold axis. (2) Atoms S(3) of **1** are not disordered and their positions are well defined, but those of **2** are disordered about the threefold axis. The position of atom S(3) of **2** listed in Table II represents a maximum in the electron density of a superposition of the two types (S, SEt) of bridge atoms. Owing to this disorder no structural parameters involving S(3) of **2** are included in Table III. (3) Each Mo atom is six coordinate. In $[Mo_2Fe_6S_8(SEt)_9]^{3-}$ the bridge distances exceed those to core S(1) atoms by 0.22 Å, the core S(1)-Mo-S(1) bond angles are larger than the bridge S(3)-Mo-S(3) bond angles by 27.9°, and the local symmetry at Mo is C_{3v}. The symmetry of the core

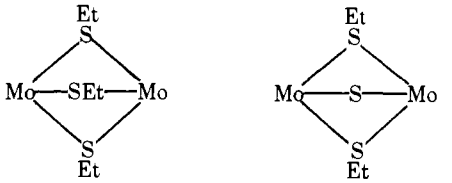

1 3.668 (4) Å **2** 3.306 (3) Å

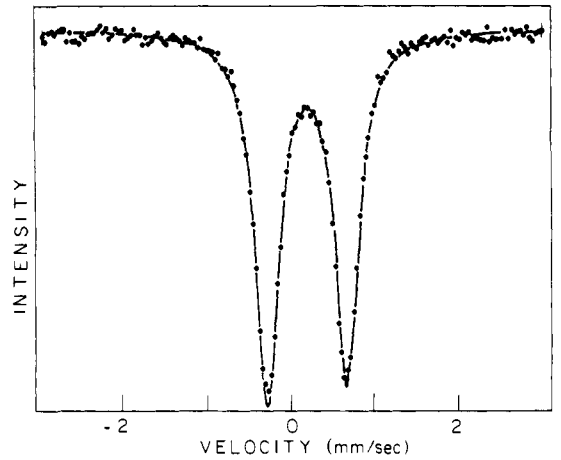

Figure 5. Mössbauer spectrum of solid $(Et_4N)_3[Mo_2Fe_6S_9(SEt)_8]$ in zero applied magnetic field at 77 K. The solid line is a theoretical fit assuming Lorentzian line shapes.

+ bridge heavy atoms of $[Mo_2Fe_6S_8(SEt)_9]^{3-}$ is C_{3h}. (4) The corresponding symmetry of $[Mo_2Fe_6S_9(SEt)_8]^{3-}$ cannot exceed C_{2v} because of the inhomogeneous nature of bridging unit **2**. However, the anion is not substantially bent about the bridge inasmuch as atom S(2) does not exhibit unusual thermal parameters (Table II), as would be expected from the disorder about the threefold axis. (5) Dimensions of unit **1** are insignificantly different from those in $[Mo_2Fe_6S_8(SPh)_9]^{3-}$ [25] (Mo···Mo 3.685 (3) Å). Parameters of unit **2** appear somewhat more sensitive to environmental effects, as judged by the Mo···Mo separations of 3.306 (3) and 3.191 (2) Å in the Et_4N^+ and $(Et_3NCH_2Ph)^+$ salts, respectively. (6) Distance and angle parameters for the $(S(1))_3Mo(S(3))_3Mo(S(1))_3$ fragment of $[Mo_2Fe_6S_8(SEt)_9]^{3-}$, according to the Cotton-Ucko criteria,[44] exhibit substantial departures (feature (3)) from an idealized confacial bioctahedron in a manner such as to indicate the lack of attractive interactions between Mo atoms. From (4) the corresponding fragment of $[Mo_2Fe_6S_9(SEt)_8]^{3-}$ also departs from this idealized arrangement. (7) The Mo···Mo separations in **1** and **2** are much larger than those in other structurally characterized binuclear triply bridged Mo complexes; these have the bridge units **3** ($[Mo_2X_9]^{3-}$,[45] X = Cl (2.66 Å), Br (2.82 Å)), **4** ($[Mo_2O_3(SCH_2CH_2O)(oxinate)_2]$,[46] 2.63 Å), and **5** ($[Mo_2O_3(SPh)_2(S_2CNEt_2)_2]$,[47a] 2.68 Å).[47b] The same

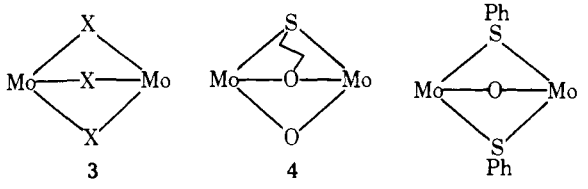

3 4 5

point applies to a number of other binuclear complexes of the type $Mo^V(\mu_2\text{-}S)_2Mo^V$ [43] and $Mo^{VI}(\mu_2\text{-}S)_2M$,[48] to $[Mo_2(\mu_2\text{-}S)_2(CN)_8]^{6-}$,[42] and to the quadruply bridged species $[(\eta^5\text{-}C_5H_5)_2Mo_2(\mu_2\text{-}SMe)_4]^{0,+}$ [49] and $[(\eta^6\text{-}MePh)_2Mo_2(\mu_2\text{-}SMe)_4]^{2+}$.[50] In these cases metal-metal distances fall in the 2.5-2.9-Å range, the bridging units usually approach planarity (excluding quadruple bridges), and weak paramagnetism or diamagnetism (where reported) is observed. While comparisons are obviously inexact, units **1** and **2**, in terms of metal-metal separations, more closely resemble the nonplanar $Mo^{IV}(\mu_2\text{-}SR)_2M$ units in $(\eta^5\text{-}C_5H_5)_2Mo(S\text{-}n\text{-}Bu)_2FeCl_2$[19] (3.66 Å) and $[((\eta^5\text{-}C_5H_5)_2Mo(SMe)_2)_2Ni]^{2+}$ [51] (3.39 Å) whose distances are not compatible with significant metal-metal bonding. On the basis of structural results, the description which emerges for $[Mo_2Fe_6S_8(SEt)_9]^{3-}$ and $[Mo_2Fe_6S_9(SEt)_8]^{3-}$ is that of two nearly isodimensional pairs of clusters in which any significant intrapair electronic coupling is more likely to be mediated by bridge atoms than to be caused by direct Mo···Mo orbital interactions.

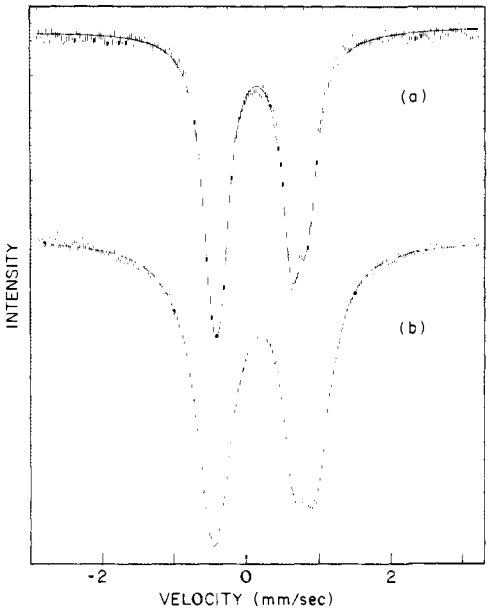

Figure 6. Mössbauer spectra of solid $(Et_3NCH_2Ph)_3[Mo_2Fe_6S_8(SEt)_9]$ in zero applied magnetic field at (a) 77 and (b) 4.2 K. The solid lines are theoretical fits assuming Lorentzian line shapes and two quadrupole doublets in each spectrum.

Table XII. Mössbauer Spectral Parameters for Mo-Fe-S Cluster Complexes

complex	T, K	δ, mm/s[a]	ΔE_Q, mm/s
$(Et_4N)_3[Mo_2Fe_6S_9(SEt)_8]$	4.2	0.28 ± 0.02	1.20 ± 0.03
	77	0.27 ± 0.02	0.95 ± 0.03
$(Et_3NCH_2Ph)_3[Mo_2Fe_6S_8(SEt)_9]$	4.2	0.28 ± 0.02	1.04 ± 0.03
		0.32 ± 0.02	1.50 ± 0.03
	77	0.27 ± 0.02	0.98 ± 0.03
		0.32 ± 0.02	1.33 ± 0.03
FeMo-co (M_{EPR})[b]	>40	0.25[c]	0.81

[a] Referenced to Fe metal at the same temperature. [b] Data from ref 21. [c] Obtained by subtracting 0.12 mm/s from the reported value of 0.37 mm/s.

Core Electron Distributions. Structural and Mössbauer Results. Attempts to provide detailed electronic descriptions of $[Mo_2Fe_6S_8(SEt)_9]^{3-}$ and $[Mo_2Fe_6S_9(SEt)_8]^{3-}$ are deferred to a subsequent report containing more extensive spectroscopic and magnetic data. Here, core electron distributions are considered in terms of the results of ^{57}Fe Mössbauer spectroscopy in zero applied magnetic field. The spectrum of $[Mo_2Fe_6S_9(SEt)_8]^{3-}$ at 77 K, shown in Figure 5, consists of a single, slightly broadened, asymmetric quadrupole doublet whose splitting and line widths increase from 77 to 4.2 K. The broadening may arise from inequivalent Fe sites owing to the presence of bridge unit **2** (structural feature (4)). The spectrum of $[Mo_2Fe_6S_8(SEt)_9]^{3-}$ at 77 K, given in Figure 6, consists of two partially resolved quadrupole doublets. Theoretical fits with unconstrained line widths, intensities, and positions indicate ca. 1:1 relative integrated intensities for the two doublets at 77 and 4.2 K. This result is inconsistent with rigorous equivalence of Fe atoms in the structure determined at ambient temperature and is being further investigated.

Spectral parameters derived from theoretical fits of the spectra assuming Lorentzian line shapes are compiled in Table

Table XIII. Summary of EXAFS Curve Fitting Results[a]

Mo-L	nitrogenase R, Å	nitrogenase no. L	$[Mo_2Fe_6S_9(SEt)_8]^{3-}$ R, Å	$[Mo_2Fe_6S_9(SEt)_8]^{3-}$ no. L	$[Mo_2Fe_6S_8(SEt)_9]^{3-}$ R, Å	$[Mo_2Fe_6S_8(SEt)_9]^{3-}$ no. L
Mo-S	2.352	3.8	2.351	3.7	2.345	2.4
Mo-Fe	2.690	2.5	2.730	2.6	2.744	2.4
Mo-S′	2.490	1.1	2.551	2.2	2.548	2.2

[a] Fits over the range of k = 4–14 Å^{-1} on Fourier filtered data. Numerical methods used in the fitting procedure are described in the Experimental Section and elsewhere.[29] The function values, $\chi = [k(\text{data fit})^2/N]^{1/2}$, for the three-wave fits of nitrogenase, $[Mo_2Fe_6S_9(SEt)_8]^{3-}$, and $[Mo_2Fe_6S_8(SEt)_9]^{3-}$ were 0.51, 0.42, and 0.37, respectively.

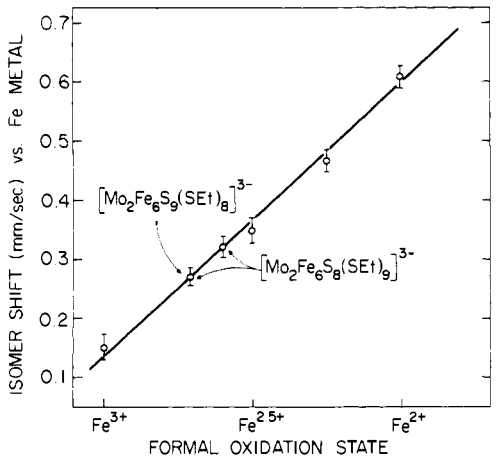

Figure 7. Dependence of isomer shifts (77 K) of ^{57}Fe in a tetrahedral sulfur environment on formal oxidation state of the metal. The line is defined by mean values of shifts of the following compounds in order of decreasing oxidation state: $[Fe(S_2\text{-}o\text{-xyl})_2]^{1-}$;[52] $[Fe_2S_2(S_2\text{-}o\text{-xyl})_2]^{2-}$;[53] $[Fe_4S_4(SR)_4]^{2-}$;[54] $[Fe_4S_4(SR)_4]^{3-}$;[37] $[Fe(S_2\text{-}o\text{-xyl})_2]^{2-}$.[52]

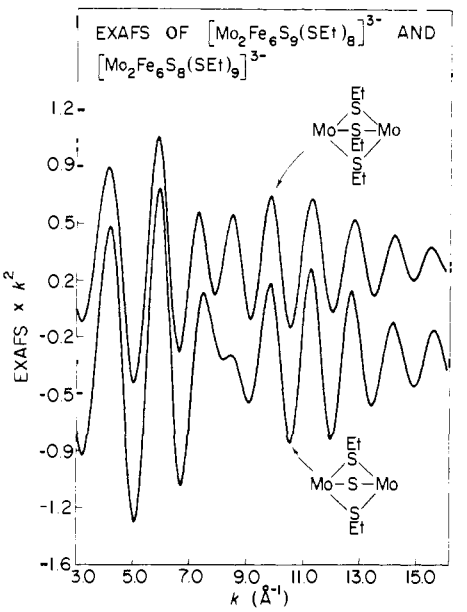

Figure 8. A comparison of the Mo EXAFS spectra of $[Mo_2Fe_6S_9(SEt)_8]^{3-}$ and $[Mo_2Fe_6S_8(SEt)_9]^{3-}$; the beat region ($k \simeq 7$–10 Å^{-1}) reflects the difference between the symmetric (**1**) and unsymmetric (**2**) bridge units.

XII. Particular interest attends the isomer shifts δ, which in discrete complexes[37,52-54] and various Fe-S phases[55] containing tetrahedral Fe-S_4 sites have been observed to vary monotonically with the formal oxidation state of the metal. A plot of δ at 77 or 4.2 K (corrected by 0.12 mm/s[56] for the second-order Doppler shift in cases of the source at ambient temperature) vs. oxidation state of synthetic analogues of Fe-S protein sites[7,16] reveals the essentially linear dependence displayed in Figure 7. Interpolation of the isomer shifts of $[Mo_2Fe_6S_8(SEt)_9]^{3-}$ and $[Mo_2Fe_6S_9(SEt)_8]^{3-}$ shows them to be closest to but smaller than the shifts of $[Fe_4S_4(SR)_4]^{2-}$ ($Fe^{+2.5}$, 2Fe(II) + 2Fe(III)) and to fall near $Fe^{2.67+}$, corresponding to a formal 2Fe(III) + Fe(II) description. This conclusion is entirely consistent with core structural feature (6) and the data in Table XI. Of these data the variations in terminal Fe-S distances are the most convincing because of the smaller standard deviations of these distances and the likelihood that they are less affected than Fe-S* (core) distances by core distortions and the replacement of a Fe by a Mo atom. The Shannon–Prewitt effective ionic radius difference, high-spin tetrahedral [Fe(II)–Fe(III)] = 0.14 Å,[57] supports assignment of a higher oxidation of Fe in $MoFe_3S_4$ cores than in $[Fe_4S_4]^{2+}$ cores. $[Mo_2Fe_6S_8(SEt)_9]^{3-}$ and $[Mo_2Fe_6S_9(SEt)_8]^{3-}$ are even- and odd-electron species, respectively. Excluding bridge S-C electron pairs these species differ by one electron. If the mean $Fe^{2.67+}$ oxidation state in both anions is accepted and cluster and bridge components are treated as EtS^- and S^{2-}, $[Mo_2Fe_6S_8(SEt)_9]^{3-}$ contains two $[Mo^{III}Fe_3S_4]^0$ cores and $[Mo_2Fe_6S_9(SEt)_8]^{3-}$ contains a $[Mo^{III}Fe_3S_4]^0$ and a $[Mo^{IV}Fe_3S_4]^+$ core, with the formal Mo oxidation states as indicated. Although the latter complex is formally mixed valence, its Mo sites are indistinguishable (symmetry related) in the crystal structure, a situation not uncommon in mixed valence species.[58] The fact that isomer shifts differ by $\leq$0.05 mm/s in the two anions indicates that electronic differences are mainly confined to bridging units **1** and **2**, even if the formal oxidation states of Mo deduced from the shifts are not accepted. Lastly, it is observed that the isomer shifts of the two anions (and, to a lesser extent, their quadrupole splittings) are comparable to the value for the M_{EPR} site in FeMo-co quoted by Rawlings et al.[21] when corrected for second-order Doppler shifts (Table XI). This result suggests a mean oxidation state near $Fe^{2.67+}$ in the EPR-active oxidation level of the cofactor.

Results of EXAFS Analyses. The Mo EXAFS spectrum of $[Mo_2Fe_6S_9(SEt)_8]^{3-}$ was recently reported[23] and was found to be similar to the spectra of two FeMo proteins[10,11] and FeMo-co[11] of nitrogenase. Analysis of the EXAFS led to the conclusion that the common structural feature is the existence of Fe and S atoms as nearest neighbors to Mo. With the full structural characterization of a second Mo-Fe-S cluster complex, $[Mo_2Fe_6S_8(SEt)_9]^{3-}$, it is of value to examine in detail the EXAFS of both synthetic clusters in relation to that of Mo in nitrogenase.

The EXAFS spectra for $[Mo_2Fe_6S_9(SEt)_8]^{3-}$ and $[Mo_2Fe_6S_8(SEt)_9]^{3-}$ are shown in Figure 8. Even casual inspection of the data reveals certain common features, notably the large positive and negative peaks in the EXAFS at about 5 and 6.4 Å^{-1}, respectively. At these values of k, the Mo-S (core) and Mo-Fe waves are approximately in phase. The major difference occurs in the beat region of the spectrum (k = 7.0–10.0 Å^{-1}) where the symmetrically bridged complex shows a substantially greater positive excursion around k = 8.5 Å^{-1}, which results from a more inphase combination of waves from the

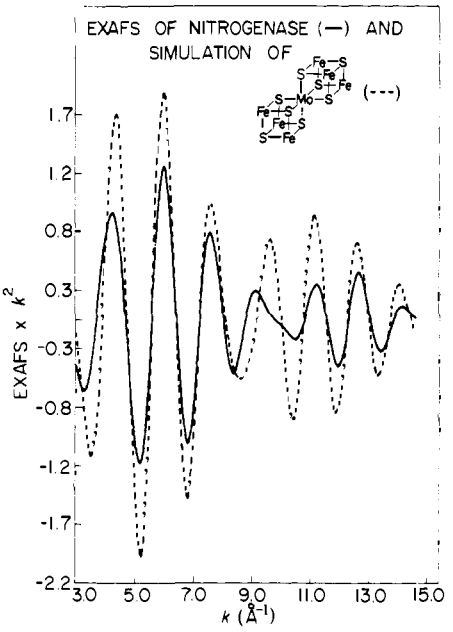

Figure 9. A comparison of the Mo EXAFS spectrum of the FeMo protein of nitrogenase of *C. pasteurianum* with a simulated spectrum of a model having the indicated $MoFe_6S_8$ core structure. The latter was obtained using semiempirical phases and amplitudes and assuming six S atoms at 2.35 Å and six Fe atoms at 2.73 Å from the Mo atom.

three core sulfide and three bridge thiolate sulfur atoms.

These results, which show visually the change in the EXAFS arising from the differences in bridge units **1** and **2** at essential parity of core structures, have been quantified by curve-fitting analysis. Fits to the data of both synthetic compounds and the FeMo protein of nitrogenase from *C. pasteurianum* have been carried out using the renormalized Mo–Fe parameters described in the Experimental Section. The results are summarized in Table XIII. The mean difference in distances determined by EXAFS compared with those for the structures reported herein is 0.007 Å while the mean error in determination of the number of coordinating atoms in each shell is 16%. The curve-fitting results and visual comparisons of EXAFS data for synthetic compounds and nitrogenase provide the best available evidence for the involvement of the Mo atom of nitrogenase in a polynuclear Mo–Fe–S cluster. Error limits in the EXAFS amplitudes do not yet permit an unambiguous characterization of the exact molecular nature of the Mo site in the enzyme. However, from comparison of the curve-fitting results for the two synthetic clusters and nitrogenase it appears unlikely that the Mo atom in a Mo–Fe–S cluster is bridged *symmetrically* to another Fe or Mo atom (e.g., as in bridging unit **1**). In this regard the conclusion from careful Mössbauer spectral analysis that the M_{EPR} center of the FeMo protein from *A. vinelandii* most probably contains 6Fe/Mo,[22] together with the finding of 6S/Mo in FeMo-co by chemical analysis,[12] permits examination of a potentially attractive model of the Mo site not yet achieved synthetically. This model, which is composed of two cubane-type cores joined by a common Mo atom ($MoFe_6S_8$),[59] is depicted in Figure 9. Also shown is an EXAFS simulated based on trigonal symmetry at Mo and distances taken from X-ray results of synthetic clusters, and the EXAFS spectrum of an FeMo protein. It may be seen that the larger number of nearest-neighbor Fe + S atoms (compared to $[Mo_2Fe_6S_8(SEt)_9]^{3-}$ or $[Mo_2Fe_6S_9(SEt)_8]^{3-}$) results in substantial disagreement of the simulated EXAFS with that of nitrogenase. In fact, the function value χ^2 (Table XIII) between this simulated data set and nitrogenase is 10.0. The value of χ^2 is a measure of the goodness of fit; a doubling of χ^2 is often taken as the criterion for statistical significance. The χ^2 for a good fit, such as that to the nitrogenase data for which the results are reported in Table XIII, is ca. 0.16–0.25. Thus, the χ^2 for this simulation is about 40-fold greater than the best fit to the nitrogenase data, leading to the conclusion that this trigonally symmetric model is an unlikely representation of the Mo environment in the enzyme. Less symmetric models based on this double cubane arrangement were not examined.

In summary, the results of EXAFS analyses lead to the conclusion that the immediate environments of Mo in nitrogenase, $[Mo_2Fe_6S_8(SEt)_9]^{3-}$, and $[Mo_2Fe_6S_9(SEt)_8]^{3-}$ are closely related and thus directly implicate Mo in the enzyme in a Mo–Fe–S cluster, The core structure of this cluster unit is such as to place three or four S atoms at ~2.3 Å, two or three Fe atoms at ~2.7 Å, and one S atom at ~2.5 Å from Mo. The first two structural features are found in the synthetic $MoFe_3S_4$ cores,[60] and the longer Mo–S distance could conceivably be part of a bridge unit to an Fe or Mo atom. By the EXAFS criterion the Mo environment in $[Mo_2Fe_6S_9(SEt)_8]^{3-}$ rather than in $[Mo_2Fe_6S_8(SEt)_9]^{3-}$ more closely resembles that in the enzyme. Further elucidation of this environment in nitrogenase by EXAFS requires improved amplitude parameters and data on the enzyme of enhanced *S/N* characteristics. Additional research in progress is aimed toward the synthesis of Mo–Fe–S clusters with a Mo:Fe:S atom ratio nearer to that in FeMo-co,[11] and with Mössbauer and EPR properties which should provide criteria (in addition to EXAFS) as to closeness of structural approach to the Mo site in nitrogenase.

Acknowledgment. This research was supported by NSF Grants CHE 77-04397 and PCM 17105 in the Department of Chemistry, Stanford University, and by the National Science Foundation at the Francis Bitter National Magnet Laboratory. Synchrotron radiation beam time was provided by the Stanford Synchrotron Radiation Laboratory, supported by NSF Grant DMR-78-27498 in cooperation with the Stanford Linear Accelerator Center and the U.S. Department of Energy.

Supplementary Material Available: Crystallographic data for $(Et_3NCH_2Ph)_3[Mo_2Fe_6S_8(SEt)_9]$ and $(Et_4N)_3[Mo_2Fe_6S_9(SEt)_8]$: positional and thermal parameters for cations (Table VI); bond distances and angles in cations (Table VII); calculated hydrogen atom positions in cations (Table VIII); values of F_o^2 and F_c^2 (Tables IX and X) (11 pages). Ordering information is given on any current masthead page.

References and Notes

(1) (a) Stanford University; (b) Alfred P. Sloan Foundation Fellow, 1976–1978; (c) Francis Bitter National Magnet Laboratory.
(2) R. C. Bray and J. C. Swann, *Struct. Bonding (Berlin)*, 11, 107 (1972).
(3) V. Massey in "Iron-Sulfur Proteins", Vol. I, W. Lovenberg, Ed., Academic Press, New York, 1973, Chapter 10.
(4) R. C. Bray in "The Enzymes", Vol. XII, Part B, P. D. Boyer, Ed., Academic Press, New York, 1975, Chapter 6.
(5) E. I. Stiefel, *Prog. Inorg. Chem.*, **22**, 1 (1977).
(6) For recent reviews of this technique cf. P. M. Eisenberger and B. M. Kincaid, *Science*, **200**, 1441 (1978); S. P. Cramer and K. O. Hodgson, *Prog. Inorg. Chem.*, in press.
(7) R. H. Holm, *Acc. Chem. Res.*, **10**, 427 (1977).
(8) T. D. Tullius, D. M. Kurtz, Jr., S. D. Conradson, and K. O. Hodgson, *J. Am. Chem. Soc.*, **101**, 2776 (1979).
(9) S. P. Cramer, H. B. Gray, and K. V. Rajagopalan, *J. Am. Chem. Soc.*, **101**, 2772 (1979).
(10) S. P. Cramer, K. O. Hodgson, W. O. Gillum, and L. E. Mortenson, *J. Am. Chem. Soc.*, **100**, 3398 (1978).
(11) S. P. Cramer, W. O. Gillum, K. O. Hodgson, L. E. Mortenson, E. I. Stiefel, J. R. Chisnell, W. J. Brill, and V. K. Shah, *J. Am. Chem. Soc.*, **100**, 3814 (1978).
(12) V. K. Shah and W. J. Brill, *Proc. Natl. Acad. Sci. U.S.A.*, **74**, 3249 (1977).
(13) W. H. Orme-Johnson and L. C. Davis in "Iron-Sulfur Proteins", Vol. III, W. Lovenberg, Ed., Academic Press, New York, 1977, Chapter 2.
(14) J. L. Johnson, H. P. Jones, and K. V.Rajagopalan, *J. Biol. Chem.*, **252**, 4994 (1977).
(15) P. T. Pienkos, V. K. Shah, and W. J. Brill, *Proc. Natl. Acad. Sci. U.S.A.*, **74**, 5468 (1977).
(16) R. H. Holm and J. A. Ibers in ref 13, Chapter 7.
(17) A. Müller, E. Ahlborn, and H.-H. Heinsen, *Z. Anorg. Allg. Chem.*, **386**, 102 (1971); A. Müller and S. Sarkar, *Angew. Chem., Int. Ed. Engl.*, **16**, 705 (1977).

(18) A. R. Dias and M. L. H. Green, *J. Chem. Soc., Chem. Commun.*, 962 (1969); *J. Chem. Soc. A*, 2807 (1971).
(19) T. S. Cameron and C. K. Prout, *Acta Crystallogr., Sect. B*, **28**, 453 (1972).
(20) P. C. H. Mitchell and D. A. Parker, *J. Chem. Soc., Dalton Trans.*, 1821 (1976).
(21) J. Rawlings, V. K. Shah, J. R. Chisnell, W. J. Brill, R. Zimmerman, E. Münck, and W. H. Orme-Johnson, *J. Biol. Chem.*, **253**, 1001 (1978).
(22) B. H. Huynh, E. Münck, and W. H. Orme-Johnson, *Biochim. Biophys. Acta*, **527**, 192 (1979).
(23) T. E. Wolff, J. M. Berg, C. Warrick, K. O. Hodgson, R. H. Holm, and R. B. Frankel, *J. Am. Chem. Soc.*, **100**, 4630 (1978).
(24) G. Christou, C. D. Garner, and F. E. Mabbs, *Inorg. Chim. Acta*, **28**, L189 (1978).
(25) (a) G. Christou, C. D. Garner, F. E. Mabbs, and T. J. King, *J. Chem. Soc., Chem. Commun.*, 740 (1978). (b) Note added in proof. The preparative method together with the structure of $[Mo_2Fe_6S_8(SCH_2CH_2OH)_9]^{3-}$ have recently been published: G. Christou, C. D. Garner, F. E. Mabbs, and M. G. B. Drew, *ibid.*, 91 (1979).
(26) G. Krüss, *Justus Liebigs Ann. Chem.*, **225**, 6 (1884).
(27) M. A. Bobrik, K. O. Hodgson, and R. H. Holm, *Inorg. Chem.*, **16**, 1851 (1977). This paper contains a listing of the computer programs used in the X-ray diffraction investigations reported here.
(28) See paragraph at end of paper regarding supplementary material.
(29) S. P. Cramer, K. O. Hodgson, E. I. Stiefel, and W. E. Newton, *J. Am. Chem. Soc.*, **100**, 2748 (1978).
(30) T. E. Wolff, J. M. Berg, P. P. Power, K. O. Hodgson, R. H. Holm and R. B. Frankel, submitted for publication.
(31) B. A. Averill, T. Herskovitz, R. H. Holm, and J. A. Ibers, *J. Am. Chem. Soc.*, **95**, 3523 (1973).
(32) B. V. DePamphilis, B. A. Averill, T. Herskovitz, L. Que, Jr., and R. H. Holm, *J. Am. Chem. Soc.*, **96**, 4159 (1974).
(33) C. Y. Yang, K. H. Johnson, R. H. Holm, and J. G. Norman, Jr., *J. Am. Chem. Soc.*, **97**, 6596 (1975).
(34) L. Que, Jr., M. A. Bobrik, J. A. Ibers, and R. H. Holm, *J. Am. Chem. Soc.*, **96**, 4168 (1974).
(35) H. L. Carrell, J. P. Glusker, R. Job, and T. C. Bruice, *J. Am. Chem. Soc.*, **99**, 3683 (1977).
(36) J. M. Berg, K. O. Hodgson, and R. H. Holm, *J. Am. Chem. Soc.*, in press.
(37) E. J. Laskowski, R. B. Frankel, W. O. Gillum, G. C. Papaefthymiou, J. Renaud, J. A. Ibers, and R. H. Holm, *J. Am. Chem. Soc.*, **100**, 5322 (1978).
(38) $[Fe_4S_4(SCH_2Ph)_4]^{3-}$, with idealized C_{2v} core symmetry in its Et_4N^+ salt,[36] is the only exception.
(39) H. Schäfer, G. Schäfer, and A. Weiss, *Z. Naturforsch. B*, **19**, 76 (1964); P. A. Koz'min and Z. V. Popova, *J. Struct. Chem.*, **12**, 81 (1971).
(40) A. Müller, W. Rittner, and G. Nagarajan, *Z. Phys. Chem. (Frankfurt am Main)*, **54**, 229 (1967); K. H. Schmidt and A. Müller, *Coord. Chem. Rev.*, **14**, 115 (1974).
(41) R. G. Dickinson and L. Pauling, *J. Am. Chem. Soc.*, **45**, 1466 (1923).
(42) M. G. B. Drew, P. C. H. Mitchell, and C. F. Pygall, *Angew. Chem., Int. Ed. Engl.*, **15**, 784 (1976).
(43) G. Bunzey and J. H. Enemark, *Inorg. Chem.*, **17**, 682 (1978).
(44) F. A. Cotton and D. C. Ucko, *Inorg. Chim. Acta*, **6**, 161 (1972). The following are the calculated (ideal) parameters (defined in this reference): d'/d'', 1.80 (1.00); $\beta - 70.53°$, 20.7° (0°); $90 - \alpha'$, 15.4° (0°).
(45) R. Saillant, R. B. Jackson, W. E. Streib, K. Folting, and R. A. D. Wentworth, *Inorg. Chem.*, **10**, 1453 (1971).
(46) J. I. Gelder, J. H. Enemark, G. Wolterman, D. A. Boston, and G. P. Haight, *J. Am. Chem. Soc.*, **97**, 1616 (1975).
(47) (a) K. Yamanouchi, J. H. Enemark, J. W. McDonald, and W. E. Newton, *J. Am. Chem. Soc.*, **99**, 3529 (1977). (b) The only exception appears to be $[Mo_2Cl_3(CO)_4(P(OMe)_3)_4]^{n+}$ (3.57 Å): M. G. B. Drew and J. D. Wilkins, *J. Chem. Soc., Dalton Trans.*, 1984 (1975).
(48) $Cu(NH_4)MoS_4$: W. P. Binnie, M. J. Redman, and W. J. Mallio, *Inorg. Chem.*, **9**, 1449 (1970). $[Ni(MoS_4)_2]^{2-}$: I. Søtofte, *Acta Chem. Scand., Ser. A*, **30**, 157 (1976).
(49) N. G. Connelly and L. F. Dahl, *J. Am. Chem. Soc.*, **92**, 7470 (1970).
(50) W. E. Silverthorn, C. Couldwell, and K. Prout, *J. Chem. Soc., Chem. Commun.*, 1009 (1978).
(51) K. Prout, S. R. Critchley, and G. V. Rees, *Acta Crystallogr., Sect. B*, **30**, 2305 (1974).
(52) R. W. Lane, J. A. Ibers, R. B. Frankel, G. C. Papaefthymiou, and R. H. Holm, *J. Am. Chem. Soc.*, **99**, 84 (1977); R. B. Frankel, G. C. Papaefthymiou, R. W. Lane, and R. H. Holm, *J. Phys. (Paris)*, **37**, C6-165 (1976).
(53) W. O. Gillum, R. B. Frankel, S. Foner, and R. H. Holm, *Inorg. Chem.*, **15**, 1095 (1976).
(54) R. B. Frankel, B. A. Averill, and R. H. Holm, *J. Phys. (Paris)*, **35**, C6-107 (1974).
(55) W. M. Reiff, I. E. Grey, A. Fan, Z. Eliezer, and H. Steinfink, *J. Solid State Chem.*, **13**, 32 (1975).
(56) R. V. Pound and G. A. Rebka, Jr., *Phys. Rev. Lett.*, **4**, 274 (1960).
(57) R. D. Shannon and C. T. Prewitt, *Acta Crystallogr., Sect. B*, **25**, 925 (1969).
(58) As, e.g., in $[(H_3N)_5Ru(pyr)Ru(NH_3)_5]^{5+}$: J. K. Beattie, N. S. Hush, P. R. Taylor, C. L. Raston, and A. H. White, *J. Chem. Soc., Dalton Trans.*, 1121 (1977).
(59) This model has also been proposed by E. Münck (private communication).
(60) As pointed out previously[23] the EXAFS data do not demonstrate the presence of atom S(2) (Figures 1 and 2) at 3.9 Å from Mo, and thus are indecisive in demonstrating the existence of the complete $MoFe_3S_4$ core in the enzyme.

A Complex Reaction Product of Dimolybdenum Tetraacetate with Aqueous Hydrochloric Acid. Structural Characterization of the Hydrido-Bridged $[Mo_2Cl_8H]^{3-}$ Ion, the $[Mo(O)Cl_4(H_2O)]^-$ Ion, and an $H_5O_2^+$ Ion with an Exceptionally Short Hydrogen Bond

Avi Bino and F. Albert Cotton*

Contribution from the Department of Chemistry, Texas A&M University, College Station, Texas 77843. *Received February 9, 1979*

Abstract: From a solution prepared by dissolving $Mo_2(O_2CCH_3)_4$ in 12 M HCl and heating to 70 °C in air followed by addition of tetraethylammonium chloride, deep yellow crystals of $[(C_2H_5)_4N]_3(H_5O_2)[Mo_2Cl_8H][MoCl_4O(H_2O)]$ are slowly deposited. This compound was identified and fully characterized by X-ray crystallography. It contains three entities of structural interest. First, the diaquahydrogen ion, $H_5O_2^+$, occurs here with an O···H···O distance shorter by ca. 0.07 Å than any previously reported in this ion; indeed, at 2.34 (1) Å, it is comparable to the few shortest O···H···O bonds known. Second, the $[Mo_2Cl_8H]^{3-}$ ion, with a μ-H atom, is here found in an ordered condition and the hydrogen atom has been located and refined in one of the bridging positions; the Mo-H distances are 1.73 Å. Third, a full structural description of the [*trans*-$MoCl_4O(H_2O)]^-$ ion is given. The Mo=O distance is 1.66 (1) Å while Mo—OH_2 is 2.33 (1) Å. This remarkable compound forms orthorhombic crystals, space group *Pnma*, with $a = 26.785$ (7) Å, $b = 10.454$ (2) Å, $c = 16.874$ (4) Å, $V = 4725$ (2) Å^3, and $Z = 4$. Using 1868 reflections having $I > 3\sigma(I)$ the structure was refined to discrepancy indices of $R_1 = 0.046$ and $R_2 = 0.064$ and a goodness-of-fit index of 1.35.

Introduction

In the first structural-chemical studies of reactions of the quadruply bonded dimolybdenum tetraacetate with aqueous hydrochloric acid the desired result was the preparation and characterization of the $[Mo_2Cl_8]^{4-}$ ion, and this was accomplished about 10 years ago by a suitable choice of reaction conditions.[1] It was noted at the same time that under other

0002-7863/79/1501-4150$01.00/0